Available online at www.sciencedirect.com
ScienceDirect
Journal of Sound and Vibration 310 (2008) 169–183
JOURNAL OF SOUND AND VIBRATION
www.elsevier.com/locate/jsvi

Thermal buckling and vibration behavior of multi-layer rectangular viscoelastic sandwich plates

V. Pradeep, N. Ganesan*

Department of Mechanical Engineering, Indian Institute of Technology, Madras, Chennai 600 036, India

Received 4 July 2007; accepted 28 July 2007
Available online 25 October 2007

Abstract

The present work deals with the thermal buckling and vibration behavior of multi-layer rectangular viscoelastic sandwich plates. A decoupled thermo-mechanical analysis is made by using finite element method. An all side clamped (**C**–**C**–**C**–**C**) plate under thermal loads is analyzed for thermal buckling, frequency and damping behavior. The temperature-dependent characteristics of complex shear modulus of viscoelastic core are accounted. The formulation proposed by Kathua and Cheung [Bending and vibration of multi-layer sandwich beams and plates, *International Journal for Numerical Methods in Engineering* 6 (1973) 11–24] has been extended to study the thermal buckling and for predicting the critical buckling temperature of the multi-layer viscoelastic sandwich plates. The variation of natural frequency and loss factor with temperature has been studied. A parametric study is conducted to estimate the effect of core thickness and progressive sandwiching. Several interesting phenomenon like shifting of modes with temperature, decrease of membrane stiffness with the increase in core thickness and increase in level of sandwiching has been observed.

1. Introduction

Sandwich structures are heavily used as subcomponents in airplane, space craft and missile structures. Sandwich structures with viscoelastic cores are particularly useful in suppressing vibration over a wide frequency range. Khatua and Cheung [1] have presented a displacement-based finite element formulation for bending and vibration of multi-layer sandwich beams and plates with orthotropic cores. Their formulation is based on classical laminate theory. Khatua and Cheung [2] applied the finite element method reported in their earlier work [1] for the stability analysis of multi-layer plates and beams. Chan and Foo [3] developed a finite strip method for the stability analysis of multi-layer sandwich plates. Alam and Asani [4] derived the governing equations of motion for vibrations of general multi-layer plate by using variational principle. In their numerical study the core is assumed to be viscoelastic and the complex modulus approach is used to model the viscoelastic behavior. Ko and Jackson [5] conducted a combined inplane and shear buckling analysis of rectangular sandwich panels under different thermal environments using Raleigh–Ritz method. Xia and Lukasiewicz [6] have studied the effect of temperature on the damping properties of the sandwich

*Corresponding author.
E-mail address: nganesan@iitm.ac.in (N. Ganesan).

0022-460X/$ - see front matter © 2007 Elsevier Ltd. All rights reserved.
doi:10.1016/j.jsv.2007.07.083

Nomenclature

a, b	half the element length and width, respectively
$[B]$	strain displacement matrix
$[B_g]$	nonlinear strain displacement matrix
$[D]$	material property matrix
$[F_{\text{th}}]^e$	element thermal load vector
G	complex shear modulus
G^*	real part of shear modulus
h_j	thickness of the jth core layer
$[K]^e$	complex element stiffness matrix
$[K_g]^e$	element geometric stiffness matrix
$[K_I]^e$	imaginary part of the complex element stiffness matrix
$[K_R]^e$	real part of the complex element stiffness matrix
$[M]^e$	element mass matrix.
n	total number of stiff layers
$[N]$	matrix of shape functions
N_{xi}, N_{yi}	stress resultants of ith stiff layer in x and y directions
$[P]$	mass density matrix
t_i	thickness of the ith stiff layer
u_i, v_i	displacements of stiff layers in x and y directions, respectively
w, θ_x, θ_y	vertical displacement and rotations in x and y directions, respectively
α_{xi}, α_{yi}	coefficient of thermal expansions of ith stiff layer in x and y directions respectively
$\gamma_{xzj}, \gamma_{yzj}$	transverse shears in jth core layer
$\{\delta\}^e$	array of nodal displacements
ΔT	temperature change
$\{\varepsilon\}$	array of strains
$\{\varepsilon\}^L$	vector of nonlinear strains
$\{\varepsilon_0\}$	free expansion thermal strains
η	material loss factor
η_i	modal loss factor
λ	buckling parameter
$[\sigma_0]^e$	array of element initial stresses
$\{\phi_i\}$	ith mode eigenvector
ω	natural frequency

structure. Kung and Singh [7] have developed a new energy-based approach for predicting the vibration and damping characteristics of a rectangular plate with multiple viscoelastic patches. Hu and Haung [8] derived the governing equations for a general 3-layer viscoelastic structure with viscoelastic core. Kant and Babu [9] have presented a finite element model using first-order and higher-order shear-deformable models for the thermal buckling of skew fiber-reinforced composite and sandwich plates. Meunier and Shenoi [10] introduced the dynamic constitutive material properties into the analytical model using elastic–viscoelastic model. The governing differential equations are solved to obtain the natural frequencies and loss factors of the composite sandwich plates including the frequency-dependent effects of the material parameters. Yu and Huang [11] derived the governing equations for a 3-layer sandwich circular plate. Recently, Matsunaga [12] has presented a two-dimensional higher-order deformation theory for thermal buckling of cross-ply laminated composite and sandwich plates. From the literature it is evident that many authors have considered the frequency-dependent characteristics of the viscoelastic materials presented in the structure. But very few works deal with the temperature-dependent characteristics of the viscoelastic material [12]. It is clear that there has been no work reported on the thermal buckling and vibration of multi-layer plates considering the temperature-dependent characteristic of viscoelastic material. Hence, the present study aims at filling this gap by developing a finite element formulation for carrying out the thermal buckling and vibration analysis of multi-layer sandwich plates. The present formulation for thermal buckling is an extension of the formulation presented by Khatua and Cheung [2] for buckling under mechanical loading. The temperature-dependent characteristics of complex shear modulus value of the viscoelastic core are accounted. Since now stiffness matrix is temperature dependent, an iterative procedure has to be adopted for carrying out thermal buckling analysis. Critical buckling temperature values are reported for **C–C–C–C** sandwich plates. A parametric study is conducted with core thickness, and number of layers as a parameter. The variation of natural frequency and loss factor with temperature is reported. Several interesting phenomena like shifting of modes with temperature, decrease of membrane stiffness with the increase in core thickness and increase in level of sandwiching have been observed. In the section to follow finite element formulation is presented.

2. Finite element formulation

The assumptions made in the finite element formulation are the following:

(1) the core is relatively soft and viscoelastic with temperature-dependent complex shear modulus $G(T) = G^*(T)(1 + i\eta(T))$;
(2) the dissipation in the core is only due to transverse shear;
(3) the transverse shear in the stiff layers is neglected;
(4) the temperature rise in the core due to dissipation of the shear stress is neglected;
(5) steady-state temperature field is assumed throughout the analysis.

The current finite element formulation is based on the classical laminate theory. The formulation presented in the work of Khatua and Cheung [1] has been extended to characterize the vibration and buckling behavior of the viscoelastic sandwich plates under thermal environment. Even though the expressions for stiffness and mass matrices are well known, they are presented for the sake of continuity.

Fig. 1 shows a rectangular multi-layer sandwich plate element. The degrees of freedom are $\{\delta_j\} = \{w \quad \theta_x \quad \theta_y \quad u_1 \quad v_1 \quad \ldots \quad u_i \quad \ldots \quad v_i \quad u_n \quad v_n\}_j$ for any node j. The array of nodal degrees of freedom is given by

$$\{\delta\}^e = \{\{\delta_1\} \quad \{\delta_2\} \quad \{\delta_3\} \quad \{\delta_4\}\}. \tag{1}$$

The displacement field within the element $\{w, \quad u_i, \quad v_i\}^T$ is related to the nodal degrees of freedom by the following expression:

$$\begin{Bmatrix} w \\ u_i \\ v_i \end{Bmatrix} = [N]\{\delta\}^e, \tag{2}$$

where $[N]$ is the shape function matrix.

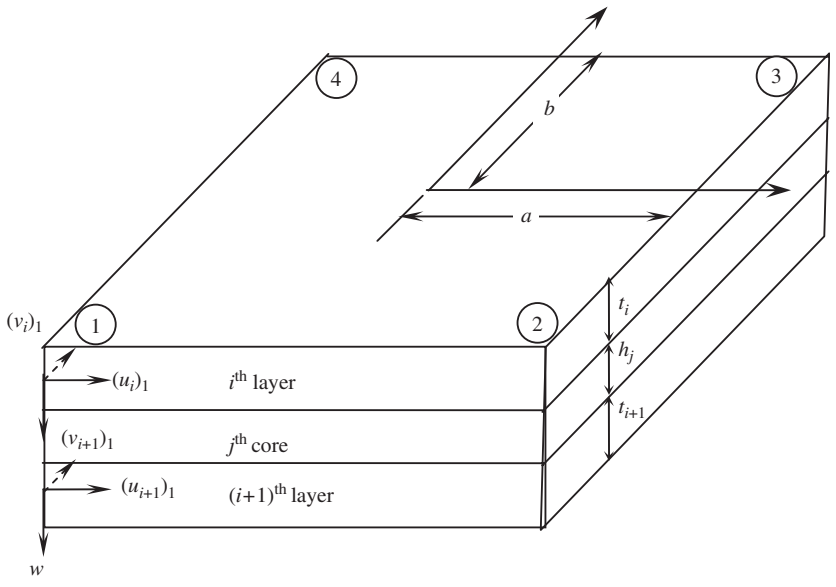

Fig. 1. Multi-layer sandwich plate element.

The array of strains $\{\varepsilon\}$ is given by

$$\{\varepsilon\} = \left\{ -\frac{\partial^2 w}{\partial x^2}, \quad -\frac{\partial^2 w}{\partial y^2}, \quad 2\frac{\partial^2 w}{\partial x\,\partial y}, \quad \frac{\partial u_1}{\partial x}, \quad \frac{\partial v_1}{\partial y}, \quad \frac{\partial u_1}{\partial y}+\frac{\partial v_1}{\partial x}, \quad \gamma_{xz1}, \quad \gamma_{yz1}, \quad \ldots, \right.$$
$$-\frac{\partial^2 w}{\partial x^2}, \quad -\frac{\partial^2 w}{\partial y^2}, \quad 2\frac{\partial^2 w}{\partial x\,\partial y}, \quad \frac{\partial u_i}{\partial x}, \quad \frac{\partial v_i}{\partial y}, \quad \frac{\partial u_i}{\partial y}+\frac{\partial v_i}{\partial x}, \quad \gamma_{xzj}, \quad \gamma_{yzj}, \quad \ldots,$$
$$\left. \gamma_{xz(n-1)}, \quad \gamma_{xz(n-1)}, \quad -\frac{\partial^2 w}{\partial x^2}, \quad -\frac{\partial^2 w}{\partial y^2}, \quad 2\frac{\partial^2 w}{\partial x\,\partial y}, \quad \frac{\partial u_n}{\partial x}, \quad \frac{\partial v_n}{\partial y}, \quad \frac{\partial u_n}{\partial y}+\frac{\partial v_n}{\partial x} \right\}. \tag{3}$$

The strains can be related to the nodal degrees of freedom by the following relation:

$$\{\varepsilon\} = [B]\{\delta\}^e, \tag{4}$$

where $[B]$ is the strain displacement matrix.

2.1. Stiffness and mass matrices

The stiffness and mass matrices can be computed by the well known formulae given by [1]

$$[K]^e = \int_{-b}^{b}\int_{-a}^{a} [B]^{\mathrm{T}}[D][B]\,\mathrm{d}x\,\mathrm{d}y, \tag{5}$$

$$[M]^e = \int_{-b}^{b}\int_{-a}^{a} [N]^{\mathrm{T}}[P][N]\,\mathrm{d}x\,\mathrm{d}y. \tag{6}$$

Since the shear modulus of the core is complex, the element stiffness matrix $[K]^e$ is a complex matrix and can be written as

$$[K]^e = [K_R]^e + [K_I]^e. \tag{7}$$

$[K_R]^e$, $[K_I]^e$ are the real and imaginary parts of the stiffness matrix $[K]^e$ respectively. $[D]$ is the property matrix and $[P]$ is the mass density matrix.

2.2. Thermal load vector and geometric stiffness matrix

The expression for thermal load vector is given by

$$[F_{\mathrm{th}}]^e = \int_{-b}^{b}\int_{-a}^{a} [B]^{\mathrm{T}}[D]\{\varepsilon_0\}\,\mathrm{d}x\,\mathrm{d}y, \tag{8}$$

where $\{\varepsilon^0\}$ are the free expansion thermal strains given by

$$\{\varepsilon_0\} = \left\{ 0 \quad 0 \quad 0 \quad \alpha_{x1}\Delta T \quad \alpha_{y1}\Delta T \quad 0 \quad 0 \quad 0 \quad \ldots, 0 \quad 0 \quad 0 \quad \alpha_{xi}\Delta T \quad \alpha_{yi}\Delta T \quad 0 \quad 0 \quad 0 \quad \ldots, \right.$$
$$\left. 0 \quad 0 \quad 0 \quad \alpha_{xn}\Delta T \quad \alpha_{yn}\Delta T \quad 0 \quad 0 \quad 0 \right\}. \tag{9}$$

α_{xi}, α_{yi} are the coefficients of thermal expansions of the ith layer in x and y directions, respectively, and ΔT is the temperature above the ambient. In the present work the two-dimensional temperature field in the plate is calculated by using 2D rectangular finite elements over the plate.

The expression for nonlinear strains $\{\varepsilon\}^L$ is given by

$$\{\varepsilon\}^L = \left\{ \left(\frac{\partial w}{\partial x}\right)^2, \left(\frac{\partial w}{\partial x}\right)^2, \ldots, n \text{ times} \right\}. \tag{10}$$

$\{\varepsilon\}^L$ can be related to the nodal degrees of freedom as

$$\{\varepsilon\}^L = [B_g]\{\delta\}^e. \tag{11}$$

The geometric stiffness matrix is given by

$$[K_g]^e = \int_{-b}^{b}\int_{-a}^{a} [B_g]^{\mathrm{T}}[\sigma_0]^e[B_g]\,\mathrm{d}x\,\mathrm{d}y, \tag{12}$$

where $[B_g]$ is the nonlinear strain displacement matrix and $[\sigma_0]^e$ is the matrix of initial stresses in the element. Expressions for $[B_g]$ and $[\sigma_0]^e$ are given in the Appendix. For the other expressions refer to Refs. [1,2].

3. Validation

The present formulation is validated for the buckling and vibration behaviors with the results existing in the literature. Since thermal buckling of multi-layer sandwich plates is not available in the literature,

Table 1
Critical buckling stresses in lb/in^2 for all side simply supported (**SS–SS–SS–SS**) sandwich plates (the geometry and material properties are given below)

Number of layers	Ref. [3] 4×4	Present number of elements			
		4×4	6×6	8×8	10×10
3	7225	7209	6984	6891	6834
5	8578	8459	8213	8100	8030
7	7613	7573	7351	7256	7197

3-layer case : $a=b=23.5$ in; $t_1=t_2=0.021$ in; $h_1=0.181$ in; $E_{x1}=E_{x2}=E_{y1}=E_{y2}=9.5\times10^6$ lb/in^2; $G_{xz1}=G_{yz1}=1.9\times10^3$ lb/in^2; $v_{x1}=v_{x2}=v_{y1}=v_{y2}=0.25$.
5-layer case : $a=b=100$ in; $t_1=t_2=t_3=0.025$ in; $h_1=h_2=0.30$ in; $E_{x1}=E_{x2}=E_{x3}=E_{y1}=E_{y2}=E_{y3}=30\times10^6$ lb/in^2; $G_{xz1}=G_{yz1}=G_{xz2}=G_{yz2}=1.9\times10^3$ lb/in^2; $v_{x1}=v_{x2}=v_{x3}=v_{y1}=v_{y2}=v_{y3}=0.25$.
7-layer case : $a=b=100$ in; $t_1=t_2=t_3=t_4=0.02$ in$h_1=h_2=h_3=0.30$ in; $E_{x1}=E_{x2}=E_{x3}=E_{x4}=E_{y1}=E_{y2}=E_{y3}=E_{y4}=30\times10^6$ lb/in^2; $G_{xz1}=G_{xz2}=G_{xz3}=G_{yz1}=G_{yz2}=G_{yz3}=1.9\times10^3$ lb/in^2; $v_{x1}=v_{x2}=v_{x3}=v_{x4}=v_{y1}=v_{y2}=v_{y3}=v_{y4}=0.25$.

Table 2
Critical stresses in lb/in^2 for a 3-layer **C–C–C–C** sandwich plate (dimensions and elastic properties are the same as in Table 1)

Stress state	Ref. [3] 4×4	Present number of elements			
		4×4	6×6	8×8	10×10
Uni-axial	17386	21704	18892	17683	17417 (16235*)
Bi-axial ($N_{xi}/N_{yi}=0.5$)	12252	14285	11904	11537	11421 (11362*)

*Series solution.

Table 3
Natural frequencies of a 5-layer **SS–SS–SS–SS** sandwich plate (the geometry and material properties are given below)

Modal m	1	2	1	3	2	3	4	1	2	4
Numbers n	1	1	2	1	2	2	1	3	3	2
Ref. [1] (5×5) in quarter plate	19	38	60	69	78	109	115	128	145	153
Present (8×8)	20	38	62	71	80	112	118	134	151	161
(10×10)	20	38	61	69	79	110	113	131	148	153

$a=72$ in; $b=48$ in; $t_1=t_2=t_3=0.011$ in; $h_1=h_2=0.125$ in; $E_{x1}=E_{x2}=E_{x3}=E_{y1}=E_{y2}=E_{y3}=10^7$ lb/in^2; $G_{xz1}=G_{xz2}=19.5\times10^3$ lb/in^2; $G_{yz1}=G_{yz2}=7.5\times10^3$ lb/in^2; $v_{x1}=v_{x2}=v_{x3}=v_{y1}=v_{y2}=v_{y3}=0.33$; $\rho_{s1}=\rho_{s2}=\rho_{s3}=259\times10^{-6}$ lb s^2/in; $\rho_{c1}=\rho_{c2}=11.4\times10^{-6}$ lb s^2/in.

the formulation is validated with the mechanical buckling results available in the literature. Table 1 compares the critical buckling stresses for the simply supported sandwich plates with those in Ref. [3]. Comparison shows that the results are in good agreement with those in Ref. [3].

Table 2 compares the critical buckling stresses for a 3-layer clamped sandwich plate. The uni-axial stress state is generated by setting α_{xi}, $v_{xi} = 0$, $i = 1, 2$. The bi-axial stress state is generated by setting $\alpha_{xi}/\alpha_{xi} = 0.5$, $v_{xi} = 0$, $i = 1, 2$. Bucking analysis is made and the corresponding critical stresses in the plate are cross verified with those reported in Ref. [3]. The results are in good agreement with the reported results.

Table 3 compares the natural frequencies of a 5-layer simply supported sandwich plate with the results reported in the literature. The results are in excellent agreement with the reported values in Ref. [1].

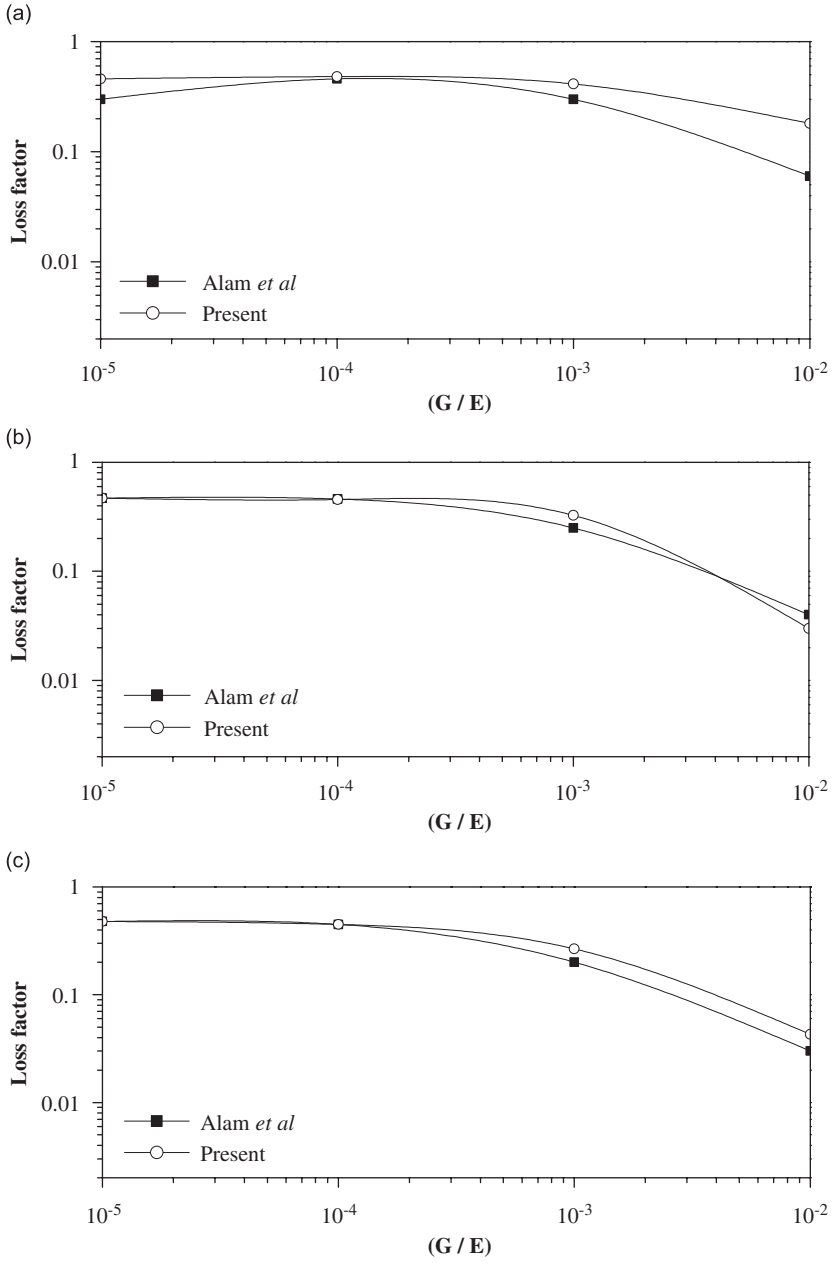

Fig. 2. Loss factors for **SS–SS–SS–SS** multi-layer sandwich plates: (a) 3-layer, (b) 5-layer, (c) 7-layer: $a/b = 1$; $T/a = 0.05$; $V = 10\rho_s/\rho_c = 2$; $\eta = 0.5$.

Fig. 2 compares the loss factor values of **SS–SS–SS–SS** multi-layer sandwich plates. The loss factor values obtained with the present formulation are in good agreement with the results available in Ref. [4].

From the above comparison studies, correctness of the formulation and computer code developed has been verified.

4. Results and discussion

4.1. Thermal buckling

The buckling temperatures of the sandwich plate can be found by solving the following eigenvalue problem:

$$[K_R]^G + \lambda[K_g]^G = 0, \tag{13}$$

where $[K_R]^G$ and $[K_g]^G$ are obtained after assembly; (refer to Eqs. (7) and (12)). The superscript G indicates global matrices. When G^* is a function of temperature, an iterative procedure has to be used to find the buckling temperature as indicated in Fig. 3. The 1st mode buckling temperature is the value of temperature

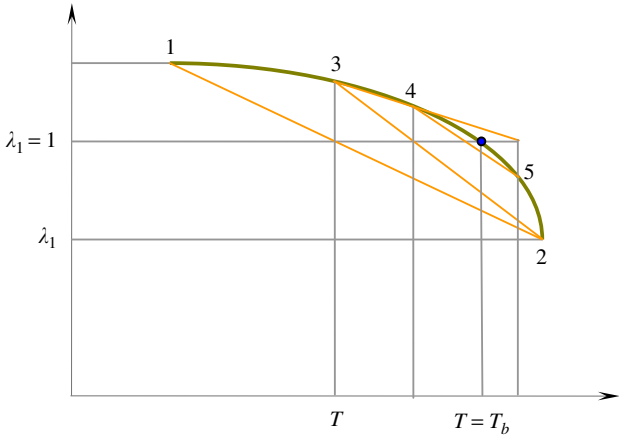

Fig. 3. Iterative algorithm for finding buckling temperatures when G^* is a function of temperature.

Table 4
Critical buckling temperatures of **C–C–C–C** sandwich plates subjected to constant temperature

Number of layers	Critical buckling temperature (°C)		
	$t_s/t_c = 2$	$t_s/t_c = 1$	$t_s/t_c = 2/3$
3	63	92	129
5	60	84	114
7	59	81	108

Table 5
Critical buckling temperatures of **C–C–C–C** sandwich plates subjected to linearly varying temperature

Number of layers	Critical buckling temperature (°C)		
	$t_s/t_c = 2$	$t_s/t_c = 1$	$t_s/t_c = 2/3$
3	95	153	223
5	89	137	196
7	87	130	184

which makes the first eigenvalue λ_1 one. The procedure starts with two initial guesses found by solving Eq. (13), namely points 1 and 2 as shown in Fig. 3. Temperature T_3, corresponding to $\lambda_1 = 1$, is found by linear interpolation or extrapolation using the points 1 and 2 and the improved guess 3 is found by re-evaluating the value of λ_1 at the temperatureT_3 by solving Eq. (13). Now 2 and 3 will be new guess points for

Table 6
Natural frequencies of the **C–C–C–C** sandwich plates at room temperature

Number of layers	Thickness ratio	Frequency (Hz)					
		Mode 1	Mode 2	Mode 3	Mode 4	Mode 5	Mode 6
3	$t_s/t_c = 2/1$	227	459	459	663	817	822
	$t_s/t_c = 1/1$	293	580	580	825	1002	1010
	$t_s/t_c = 2/3$	348	675	675	948	1138	1148
5	$t_s/t_c = 2/1$	214	437	437	543	543	637
	$t_s/t_c = 1/1$	270	541	541	541	541	645
	$t_s/t_c = 2/3$	316	539	539	624	624	642
7	$t_s/t_c = 2/1$	208	386	386	421	421	460
	$t_s/t_c = 1/1$	257	385	385	459	513	513
	$t_s/t_c = 2/3$	298	385	385	458	564	586

$a = 0.5\,\text{m}$, $b = 0.5\,\text{m}$, $t_s = 4\,\text{mm}$; G^*, η from Fig. 4; ambient temperature 30 °C.

Table 7
First six modes of **C–C–C–C** sandwich plates at room temperature (the geometry and material parameters are indicated below)

Description	Mode number					
Plate	1	2	3	4	5	6
3-Layer $t_s/t_c = 2/1$ $t_s/t_c = 1/1$ $t_s/t_c = 2/3$	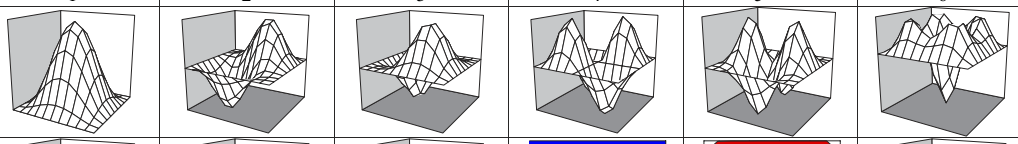					
5-Layer $t_s/t_c = 2/1$	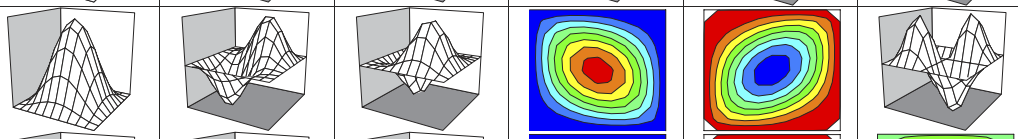					
$t_s/t_c = 1/1$	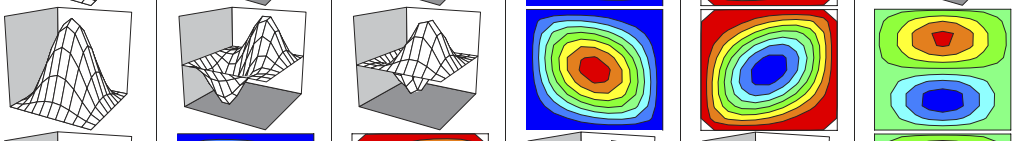					
$t_s/t_c = 2/3$	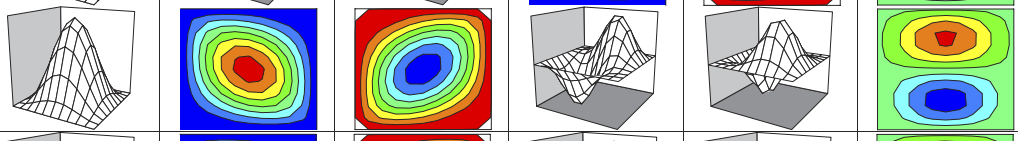					
7-Layer $t_s/t_c = 2/1$	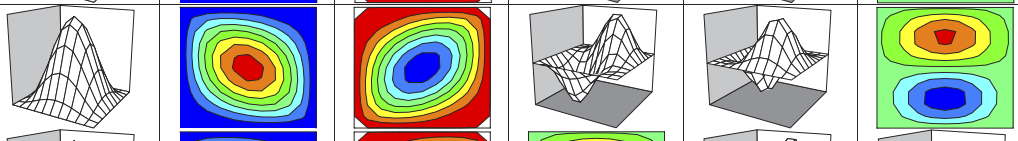					
$t_s/t_c = 1/1$ $t_s/t_c = 2/3$	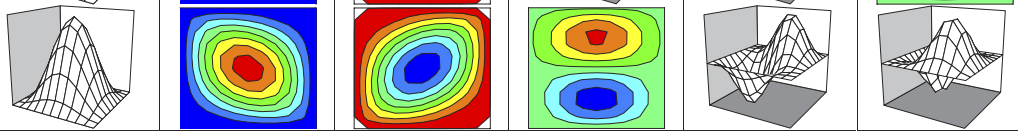					

$a = 0.5\,\text{m}$, $b = 0.5\,\text{m}$, $t_s = 4\,\text{mm}$; G^*, η from Fig. 4; ambient temperature 30 °C.

the next iteration. The procedure is repeated by using the latest two guesses till the two guesses converge to the buckling temperature T_b and $\lambda_1 = 1$.

A **C–C–C–C** plate is analyzed for buckling behavior under two different temperature fields. Table 4 gives the critical buckling temperature values for the multi-layer sandwich plates subjected to constant temperature throughout. As expected with the increase in core thickness, buckling temperature increases. Progressive sandwiching lessens the buckling temperature as shown in Table 4. Table 5 shows the critical temperature values for a clamped plate subjected to linearly varying temperature field. Temperature is held constant (30 °C) on one edge and the temperature of the other edge is varied till the bucking occurs. In this case by the word buckling temperature, we mean the temperature to be specified on the other edge at which buckling occurs.

4.2. Evaluation of natural frequency and loss factor

For finding the natural frequency of the sandwich plates the following eigenvalue problem has to be solved:

$$[K_R]^G + \omega^2[M]^G = 0, \tag{14}$$

where ω^2 is the square of natural frequency. $[K_R]^G$ and $[M]^G$ are the real part of stiffness matrix and mass matrix in a global sense (refer to Eqs. (6) and (7)). The modal loss factor η_i for any mode i can be found by

Table 8
Shift of modes with temperature case 5-layer, $t_s/t_c = 2/3$

Description	Mode number					
Temperature (°C)	1	2	3	4	5	6
30–55	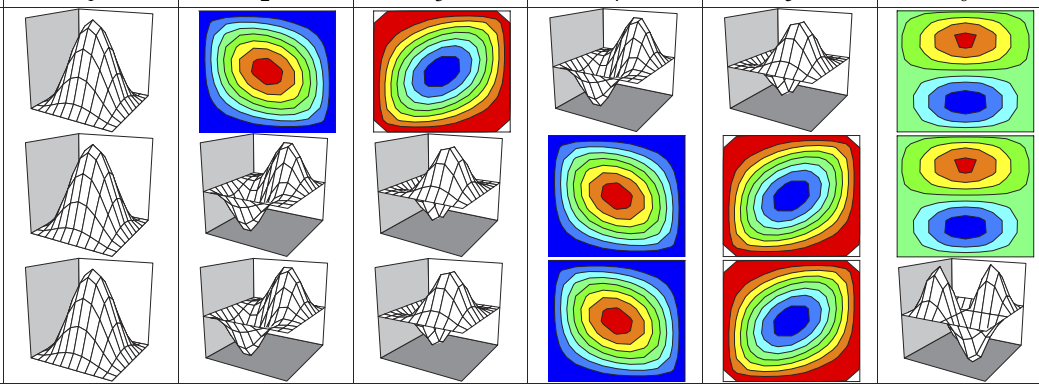					
55–85						
85–110						

$a = 0.5\,\text{m}$, $b = 0.5\,\text{m}$, $t_s = 4\,\text{mm}$, G^*, η from Fig. 4.

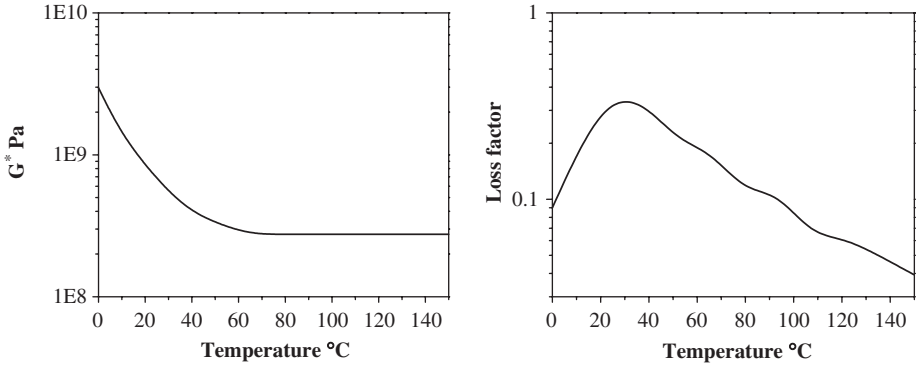

Fig. 4. Variation of shear modulus and material loss factor values with temperature for EC 2216.

using modal strain energy method by using the following equation:

$$\eta_i = \frac{\{\phi_i\}^{\mathrm{T}}[K_I]^G\{\phi_i\}}{\{\phi_i\}^{\mathrm{T}}([K_R]^G + [K_g]^G)\{\phi_i\}}, \tag{15}$$

where $\{\phi_i\}$ is the eigenvector corresponding to mode i.

4.3. Effect of core thickness and sandwiching configuration on mode shapes

Table 6 shows the first six natural frequencies of **C–C–C–C** multi-layer sandwich plates at room temperature. The corresponding mode shapes are given in Table 7. For a 3-layer sandwich plate, all the first six modes are predominantly bending modes. For a 5-layer plate with $t_s/t_c = 2/1$, the first three modes are

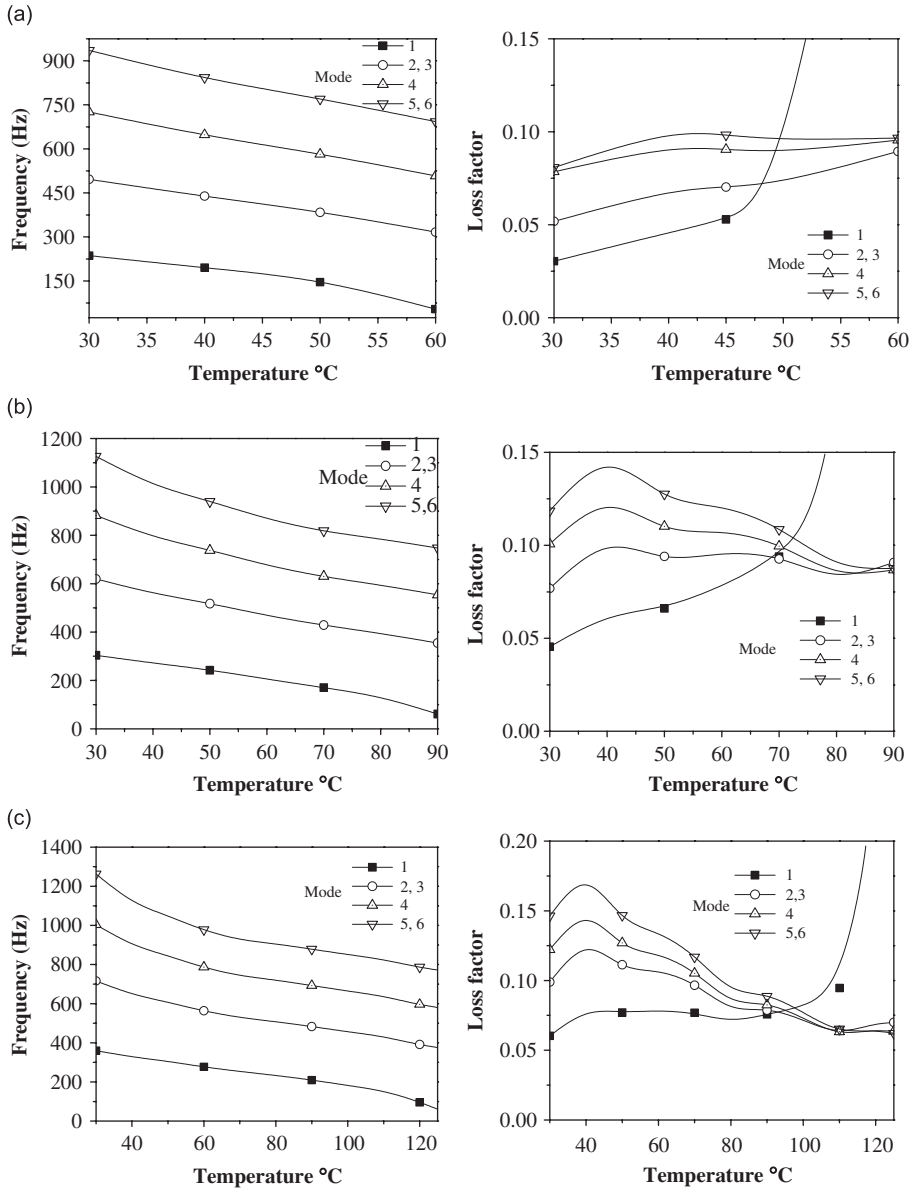

Fig. 5. Variation of frequency and loss factor with temperature for a 3-layer **C–C–C–C** sandwich plate subjected to constant temperature: (a) $t_s/t_c = 2/1$, (b) $t_s/t_c = 1/1$, and (c) $t_s/t_c = 2/3$.

predominantly bending modes. The 4th and 5th modes are pure membrane modes and the 6th mode is still a bending mode. Membrane mode shapes are symbolically shown. Only the u displacements are shown in the membrane modes. Of course the v displacement plots will also look the same. For a 5-layer plate with $t_s/t_c = 1/1$, all the modes are similar to the case of $t_s/t_c = 2/1$, except that the 6th mode is a coupled mode with predominantly membrane characteristics. For a 5-layer plate with $t_s/t_c = 2/3$, the membrane modes occur very much at the 2nd and 3rd positions, the 4th and 5th modes are bending and the 6th mode is a coupled mode. For a 7-layer plate with $t_s/t_c = 2/1$, the 1st mode is a bending mode, the 2nd and 3rd are pure membrane modes, the 4th and 5th modes are bending modes and the 6th mode is a coupled mode. For a 7-layer plate with $t_s/t_c = 1/1$ and $t_s/t_c = 2/3$, the coupled mode occupies the 4th position, and the 5th and 6th positions are occupied by the bending modes. From Table 7 it can be seen that for a given core thickness, with the increase in degree of sandwiching the membrane modes become predominant. This effect is more

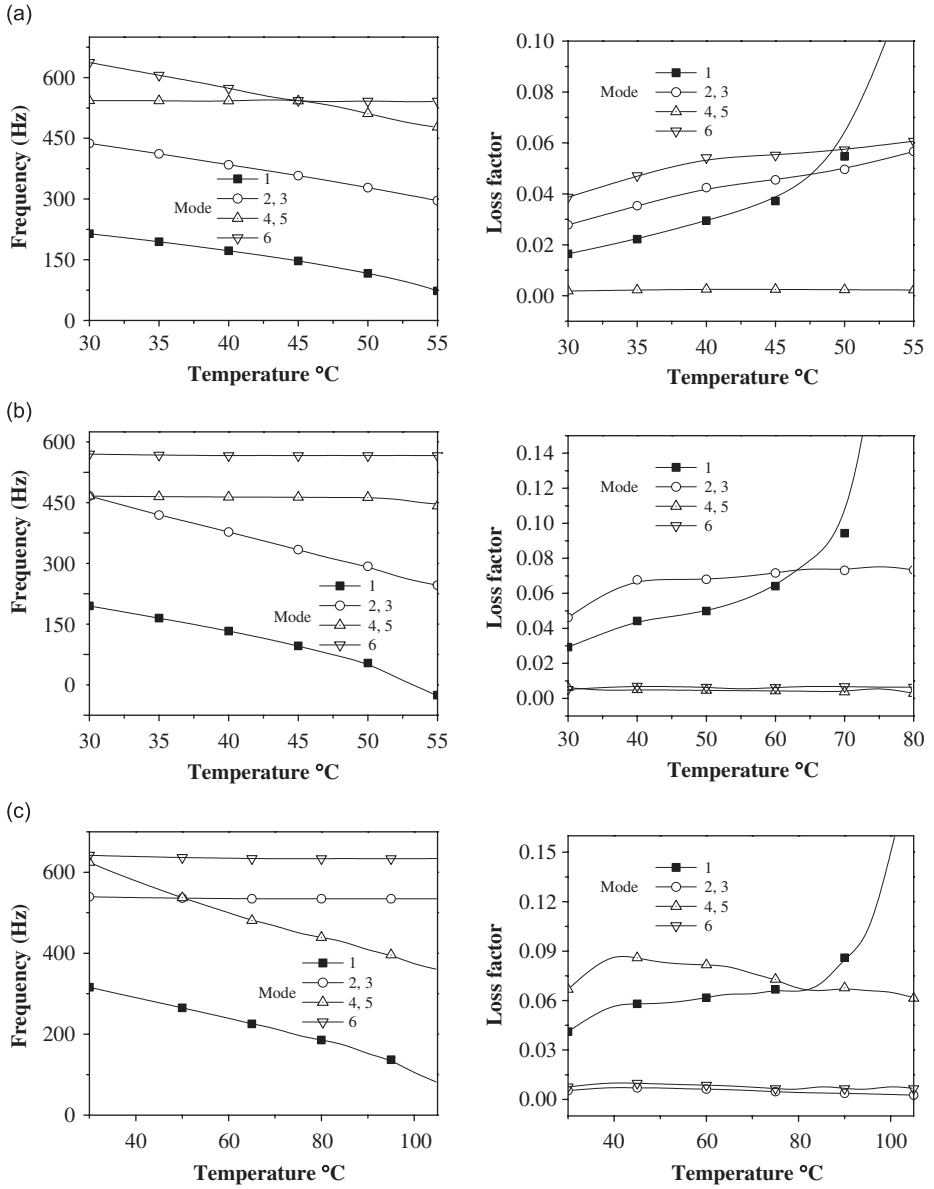

Fig. 6. Variation of frequency and loss factor with temperature for a 5-layer **C–C–C–C** sandwich plate subjected to constant temperature: (a) $t_s/t_c = 2/1$, (b) $t_s/t_c = 1/1$, and (c) $t_s/t_c = 2/3$.

prominent at the high core thickness. For a given sandwich configuration, increase in core thickness increases the bending natural frequencies to a notable degree. But the membrane frequencies will increase marginally. This is to be expected as increase in core thickness considerably increases the bending stiffness. In contrast the membrane frequency increases marginally similar to the axial vibration of a beam. For a given core thickness, the 3-layer sandwich plate has the highest frequency, indicating that this configuration is stiffer than the other ones.

4.4. Effect of temperature on mode shapes

It is observed that with the increase in temperature, the lowest frequency mode shapes get altered for the 5- and 7-layer configurations. To explain this phenomenon, a typical case of 5-layer plate with $t_s/t_c = 2/3$

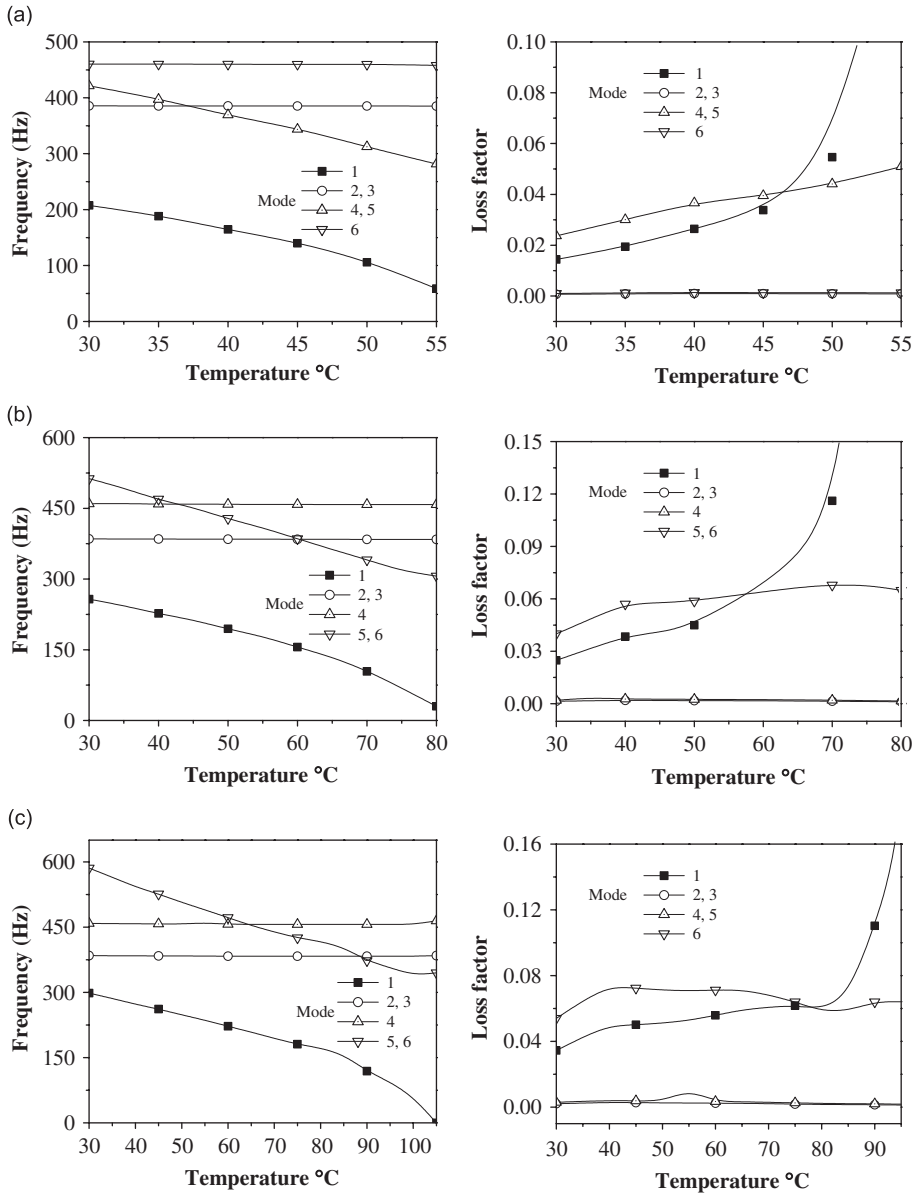

Fig. 7. Variation of frequency and loss factor with temperature for a 7-layer **C–C–C–C** sandwich plate subjected to constant temperature: (a) $t_s/t_c = 2/1$, (b) $t_s/t_c = 1/1$, and (c) $t_s/t_c = 2/3$.

is considered. Table 8 shows the shift of the mode shapes with temperature. For the plate considered the room temperature, modes will persist as lowest six modes up to 55 °C. In the range of 55–85 °C the positions of membrane modes and bending modes get interchanged. Above 85 °C the 6th mode changes to bending mode instead of being a coupled mode. With the increase in temperature the bending stiffness of the system will fall because of the addition of geometric stiffness matrix, whereas the membrane stiffness is almost unaffected with temperature. This is the reason that can be attributed to the change of mode shapes with temperature. Because of this effect while plotting the variation of temperature versus frequency, care should be taken and the room temperature modes have to be properly tracked over the temperature range of interest.

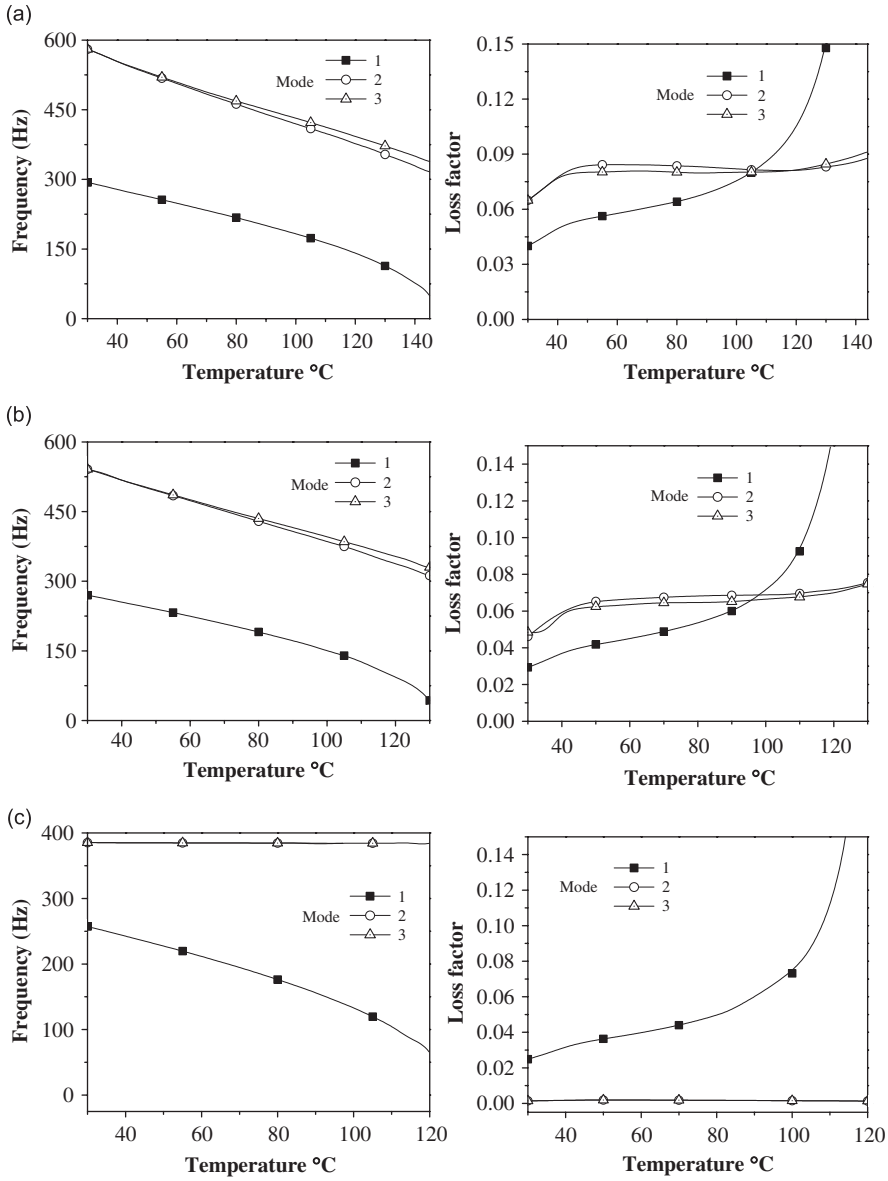

Fig. 8. Variation of frequency and loss factor with temperature for a **C–C–C–C** sandwich plate subjected to linearly varying temperature ($t_s/t_c = 1/1$): (a) 3-layer, (b) 5-layer, and (c) 7-layer.

4.5. Influence of temperature on frequency and loss factor

Fig. 4 shows the variation of shear modulus (real part G^*) and material loss factor η with temperature [13]. Figs. 5–7 show the variation of natural frequency and loss factor with temperature for a 3-, 5- and 7-layer sandwich plates, respectively. The plates are clamped on all the four edges and are subjected to constant temperature throughout the plate domain. The 1st mode frequency starts decreasing with temperature and finally falls to zero at buckling temperature. The corresponding loss factor keeps increasing with temperature and drastically increases near the buckling temperature. The frequency of all the bending modes tends to decrease with temperature. The corresponding loss factor values follow a hill-shaped curve. The reason for this is the overlapping of geometric stiffness effect and variation of material loss factor with temperature. Referring to the expression for modal loss factor η_i (refer to Eq. (15)), the denominator of the expression will go on decreasing with temperature due to the addition of geometric stiffness matrix. The numerator, since it entirely depends on material loss factor, will vary in the same manner as the material loss factor does with temperature. The influence of geometric stiffness matrix is felt more in the 1st mode. From Fig. 4 it can be seen that the material loss factor has got a maximum value at around 40 °C. Correspondingly a maxima in loss factor can be seen at around 40 °C from Figs. 5–7 for all the bending modes. The core thickness will always increase the damping. There is a little influence of temperature on the membrane modes. Further, there is a little contribution from the membrane modes to the damping of the system. Fig. 8 shows the variation of frequency and loss factor of sandwich plates subjected to linearly varying temperature. One edge of the plate is held at constant temperature. The variations of frequency and loss factor with the temperature of the other edge are plotted.

Appendix

$$
\begin{aligned}
[B_g] &= \left[\{B_1\}, \quad \{B_2\}, \quad \ldots \quad \{B_i\}, \quad \ldots \quad \{B_n\}\right]^{\mathrm{T}},\\
\{B_i\} &= \left\{\{A_1\} \quad \{A_2\} \quad \{A_3\} \quad \{A_4\}\right\},\\
\{A_k\} &= \left\{N_{k1,x} \quad N_{k2,x} \quad N_{k3,x} \quad \vdots \quad 2n \text{ zeros}\right\},
\end{aligned}
$$

where x indicates derivative with respect to x and N_{ki} are the shape functions [1].

$$
[\sigma_0]^e = \begin{bmatrix}
[N]_1 & & & & & \\
& [N]_2 & & & & \\
& & \ddots & & & \\
& & & [N]_i & & \\
& & & & \ddots & \\
& & & & & [N]_n
\end{bmatrix} \quad \text{where } [N]_i = \begin{bmatrix} N_{xi} & 0 \\ 0 & N_{yi} \end{bmatrix}.
$$

References

[1] T.P. Khatua, Y.K. Cheung, Bending and vibration of multilayer sandwich beams and plates, *International Journal for Numerical Methods in Engineering* 6 (1973) 11–24.

[2] T.P. Khatua, Y.K. Cheung, Stability analysis of multilayer sandwich structures, *AIAA Journal* 9 (1973) 1233–1234.

[3] H.C. Chan, O. Foo, Buckling of multi-layer sandwich plates by the finite strip method, *International Journal of Mechanical Sciences* 19 (1977) 447–456.

[4] N. Alam, N.T. Asani, Vibration and damping analysis of multilayered rectangular plates with constrained viscoelastic layers, *Journal of Sound and Vibration* 97 (4) (1984) 597–614.

[5] W.L. Ko, R.H. Jackson, Compressive and shear buckling analysis of metal matrix composite sandwich panels under different thermal environments, *Composite Structures* 25 (1993) 227–239.

[6] Z.Q. Xia, S. Lukasiewicz, Effect of temperature changes on damping properties of sandwich cylindrical panels, *International Journal of Solids and Structures* 33 (6) (1996) 835–849.
[7] S.W. Kung, R. Singh, Complex eigensolutions of rectangular plates with damping patches, *Journal of Sound and Vibration* 216 (1) (1998) 1–28.
[8] Y.-C. Hu, S.-C. Haung, The frequency response and damping effect of three-layer thin shell with viscoelastic core, *Computers and Structures* 76 (2000) 577–591.
[9] T. Kant, C.S. Babu, Thermal buckling analysis of skew-fiber reinforced composite and sandwich plates using shear deformable finite element models, *Composite Structures* 49 (2000) 77–85.
[10] M. Meunier, R.A. Shenoi, Dynamic analysis of composite sandwich plates with damping modeled using higher-order shear deformation theory, *Composite Structures* 54 (2001) 243–254.
[11] S.-C. Yu, S.-C. Haung, Vibration of three-layered viscoelastic sandwich circular plate, *International Journal of Mechanical Sciences* 43 (2001) 2215–2236.
[12] H. Matsunaga, Thermal buckling of cross-ply laminated composite and sandwich plates according to global higher-order deformation theory, *Composite Structures* 68 (2005) 439–454.
[13] A.D. Nashif, D.I.G. Jones, J.P. Henderson, *Vibration Damping*, first ed, Wiley, New York, 1985.